Bioorganic & Medicinal Chemistry Letters 21 (2011) 4891–4899

Contents lists available at ScienceDirect

Bioorganic & Medicinal Chemistry Letters

journal homepage: www.elsevier.com/locate/bmcl

6-Aryl-3-pyrrolidinylpyridines as mGlu5 receptor negative allosteric modulators

Jesse M. Weiss [a], Hermogenes N. Jimenez [a], Guiying Li [a,*], Myriam April [a], Michelle A. Uberti [b], Maria D. Bacolod [a], Robb M. Brodbeck [b], Darío Doller [a,*]

[a] Chemical & Pharmacokinetic Sciences, Lundbeck Research USA, 215 College Road, Paramus, NJ 07652, USA
[b] Synaptic Transmission Disease Biology Unit, Lundbeck Research USA, 215 College Road, Paramus, NJ 07652, USA

ARTICLE INFO

Article history:
Received 24 May 2011
Revised 3 June 2011
Accepted 6 June 2011
Available online 17 June 2011

Keywords:
mGlu5 NAM
Metabotropic glutamate receptors
GPCR
mGluR
CNS drug discovery

ABSTRACT

A series of 6-aryl-3-pyrrolidinylpyridine analogs was explored as structurally novel negative allosteric modulators of the mGlu5 receptor lacking an alkyne or oxadiazole moiety. Compounds in this series were characterized by tractable SAR, good in vitro potencies and brain penetration in rodents.

L-Glutamic acid (**1**) is the major excitatory neurotransmitter in the mammalian central nervous system and is responsible for a variety of physiological effects acting through a number of receptors.[1] These receptors are either *ionotropic* (iGluRs) or *metabotropic* glutamate receptors (mGluRs). iGluRs are ion channels, and have been divided in three classes based on their selective interactions with three different ligands: *N*-methyl-D-aspartic acid (NMDA, **2**), kainic acid (KA, **3**) and (*S*)-2-amino-3-(-3-hydroxy-5-methyl-4-isoxazolyl)propionic acid (AMPA, **4**).

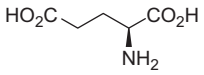

L-Glutamic acid (**1**)

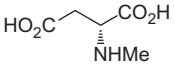

N-methyl-D-aspartic acid (NMDA, **2**)

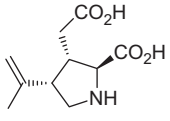

Kainic acid (KA, **3**)

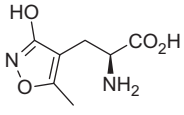

AMPA (**4**)

mGluRs, on the other hand, are coupled to a variety of second messenger systems via G proteins, thus belonging to the G-protein coupled receptor family (GPCRs). The main structural feature of all known GPCRs is their extensive amino acid sequence similarities, generating seven α-helical transmembrane domains. GPCRs have been classified into six distinct classes, identified as A–F.[2] However, from a drug discovery perspective, classes A, B and C have captured most of the efforts aimed at finding new therapeutic agents.[3]

mGluRs belong to class C of GPCRs, together with calcium-sensing receptors, $GABA_B$ receptors, and sweet taste receptors, among a variety of others. Class C GPCRs are characterized by a unique molecular pharmacology.[4] The so-called *orthosteric* ligands of mGlu receptors bind in the extracellular amino-terminal domain (Fig. 1). These ligands often suffer from poor selectivity among mGlu receptor subtypes due to a relatively highly conserved binding region across the receptor family.[5] In the past decade a number of allosteric sites, those not native to the glutamate binding site, have been identified for several of the mGlu receptors. In most cases, allosteric binding sites are thought to be in

* Corresponding authors. Tel.: +1 201 350 0341; fax: +1 201 261 0623.
E-mail address: dado@Lundbeck.com (D. Doller).

0960-894X/$ - see front matter © 2011 Elsevier Ltd. All rights reserved.
doi:10.1016/j.bmcl.2011.06.014

the seven-transmembrane spanning region of the mGlu receptors, and designing ligands that target this region is a strategy that has been demonstrated to produce selective receptor modulation.[6]

To date, eight different mGluR subtypes (mGlu1-8) have been cloned and subsequently expressed in various cell lines. The mGluRs are further subdivided into three groups based on sequence homology, second messenger coupling and pharmacology: Group 1 (mGlu1 and 5), Group 2 (mGlu2 and 3) and Group 3 (mGlu4, 6, 7 and 8). mGlu5 receptors are principally localized postsynaptically and couple primarily via activation of members of the $G_{q/11}$ family of G-proteins to phospholipase C-β and, hence, have been reported to lead to elevation of intracellular calcium ion levels.[3]

A number of reports in the literature reviewed the potential clinical use of novel mGlu5 allosteric modulators.[6,7] In the late seventies, fenobam (**5**) demonstrated clinical efficacy as an anxiolytic operating through a then unknown, non-benzodiazepine mechanism. Eventually, it was found to be a potent mGlu5 receptor NAM.[8] Although the compound did not progress into late stage trials due to poor pharmacokinetics, the efficacy demonstrated in a clinical setting propelled investigations seeking novel NAMs of the mGlu5 receptor. Research intensified upon discovery of tool compounds like MPEP (**6**) or MTEP (**7**), which have shown efficacy in a variety of preclinical models, including pain, anxiety, L-dopa induced dyskinesia (LID) and Fragile X Syndrome.[9] In addition, a number of mGlu5 NAMs have entered clinical studies and proven efficacious in indications such as migraine,[10] gastro-esophageal reflux disease (GERD),[11] Fragile X syndrome,[12] and LID.[13] Many of these compounds [e.g., ADX10059 (**8**), ADX48621 (**9**), AFQ056 (**10**)] are characterized by a disubstituted alkyne as a key component of the structural motif. The safety and toxicological properties of this moiety have been questioned for a number of reasons, not the least of which was the termination of the clinical studies of ADX10059 for chronic indications due to liver function abnormalities.[14] This and our interest in this target and its potential therapeutic value motivated us to explore novel mGlu5 chemical space lacking the alkyne functionality.

In search of novel chemotypes lacking the alkyne moiety as the central feature, the 6-aryl-3-pyrrolidinylpyridine series was investigated as a potential starting point (scaffold **A**, **11**). Conceptually, this scaffold is related to recently reported lead compounds (e.g., **12**[15a] and **13**[15b]) and evolved through a scaffold hopping exercise (Fig. 2). We reasoned that a potential advantage of the pyridine ring over the oxadiazole system is the possibility of adding substituents in the pyridine ring as a strategy leading to optimized drug candidates through potency improvements or by modulation of physicochemical/biochemical attributes. A computational overlay showed that the optimal Ar and/or Y substituents might not be identical, since they project differently into space (Fig. 3).[16]

Based on prior SAR knowledge for mGlu5 receptor NAMs,[17] the initial focus was centered on 3-chlorophenyl derivatives. Scheme 1 depicts the reaction sequence leading to analogs without substitution on C-4 of the pyridine core. Starting with 6-chloropyridine-3-carboxaldehyde **14a**, the procedure reported by Stetter et al. for the addition of aldehydes to activated double bonds yielded ketoester **15**.[18] Reductive amination followed by spontaneous cyclization afforded lactam **16**, which was submitted to a standard Suzuki coupling to yield compound **17**. Reduction to pyrrolidine **18** was accomplished in good yield with BH_3·THF complex. Acylation with an appropriate carboxylic acid in the presence of EDCI and DMAP provided compounds **11a**–**11f** (Table 1).[19]

Scheme 2 shows the reaction sequence leading to analogs with 4-methyl or 4-methoxy substitution in the pyridine ring. To that end, the appropriately substituted 6-chloropyridine-3-carboxaldehyde **14b** or **14c** (R^1 = Me or OMe, respectively) underwent a Suzuki coupling to establish the biaryl functionality of the scaffold. The aldehyde group in **19a** or **19b** was functionalized to the homoallyl azide **21a** or **21b**, respectively, via a Grignard addition of allylmagnesium bromide, followed by reactions of alcohols **20a** or **20b** with diphenylphosphoryl azide (DPPA). Treatment of intermediate azides **21a** or **21b** with dicyclohexylborane (prepared in situ) afforded the pyrrolidine **22a** or **22b**, respectively, in very good overall

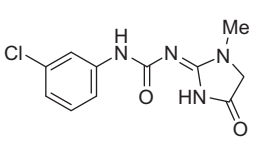

Fenobam (**5**)

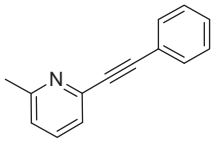

MPEP (**6**)

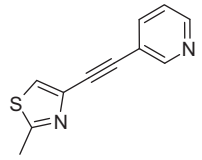

MTEP (**7**)

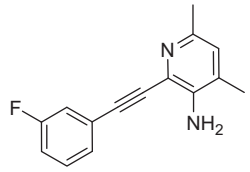

ADX10059 (**8**, Addex)

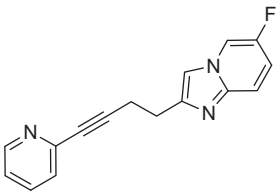

ADX48621 (**9**, Addex)

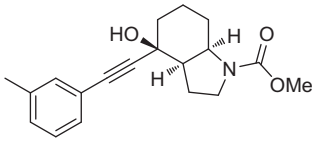

AFQ-056 (**10**, Novartis)

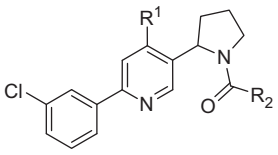

Scaffold **A** (**11**)

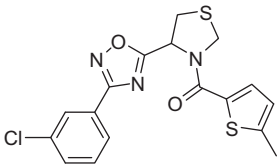

(**12**, Gedeon Richter[15a])

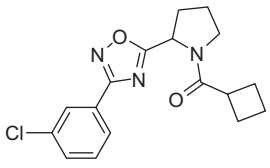

(**13**, Vanderbilt Univ. [15b])

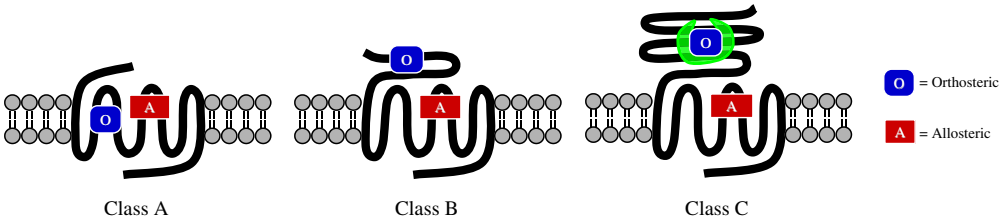

Figure 1. Schematic representations of the architecture of class A, B and C GPCRs, indicating the spatial relationship between the allosteric and the orthosteric binding sites.

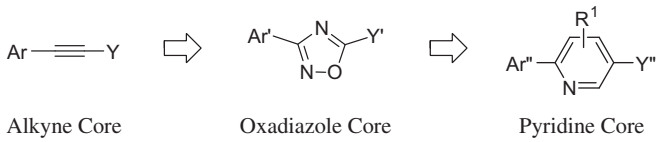

Figure 2. Series of scaffold hopping operations leading to series **A**.

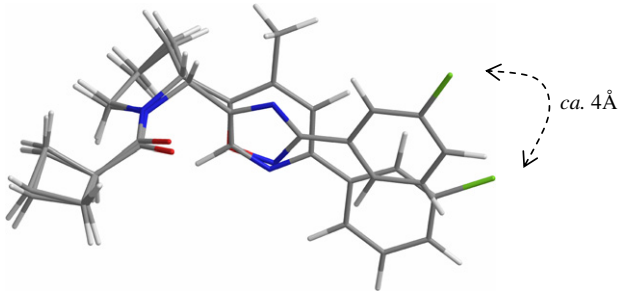

Figure 3. Low energy conformations overlay for pyridine and oxadiazole scaffolds. Cyclobutylamide analogs are exemplified. The 3-chlorophenyl groups are projected into slightly different directions, and the chlorine atoms are separated by ca. 4 Å.

yield. Finally, amide formation with the corresponding carboxylic acid afforded the desired final products in scaffold **A**.

Early SAR studies focused on the effects of modifying the amide substituent $\mathbf{R}^2$, as well as exploiting the potential impact of an $\mathbf{R}^1$ group in the 4-position of the pyridine ring on basicity and overall shape. Functional activities were measured by the ability of the compound to inhibit calcium mobilization caused by an EC_{80} concentration of glutamate in HEK293 cells expressing the human mGlu5 receptor.[20a] Binding affinities were determined via displacement by a compound of the allosteric radioligand [^{3}H]-MPEP.[20b] Values for relevant compounds are summarized in Table 1.

Pyridine analogs unsubstituted at the 4-position (**11a**–**11f**) showed excellent functional potency and potent binding, the later being ca. 10-fold shifted (vide infra). Testing of a number of cyclic amide analogs indicated that ring size of 4 or 5 was preferred over 6, with the pyrazine amide **11e** being the most potent compound among the six-membered heteroaryl amides (data not shown). Among five-membered heterocyclic rings, the 2-thiazolyl or 5-thiazolyl moieties were particularly potent (**11b** and **11c**, respectively). Polar surface areas (PSA) and *c* Log *P* values were consistent with those required for optimal design of CNS drugs.[21] However, lipophilic ligand efficiency (LLE) values were relatively low, indicating that further potency increases were needed to afford improved compounds. This was accomplished by substitution on the pyridine ring.

A methyl group on the 4-position of the pyridine ring led to a three- to four-fold enhancement in binding affinity and 4–13-fold increase in functional potency (**11h** vs **11c**, and **11i** vs **11d**). A 4-methoxy substituent had 5–30-fold increase in binding affinity (**11s** vs **11c**, and **11t** vs **11f**), but changes in functional potency were modest (one to three-fold for the same two pairs of compounds). There is precedent for such disconnects between functional and binding affinity for mGlu5 receptor allosteric modulators.[15c] These enhancements in binding affinity may reflect increases in basicity from the 4-unsubstituted core (pK_a 3.5) to the more basic 4-methyl (pK_a 4.1) and 4-methoxy (pK_a 5.0) derivatives (Table 1). The 4-hydroxypyridine **11u** and the tertiary alcohol **11v** were less potent. Five- and six-membered heterocyclic amides, as well as cyclobutyl carboxamides (**11p** and **11t**) were preferred substituents. As previously noted, among five-membered heterocycles, both 2- and 5-thiazolyl amides were preferred substituents. Alicyclic five-membered ring systems were explored, but were not tolerated (e.g., **11q**–**r**), and six-membered heteroaromatic rings were less potent, with the notable exception of the 2-pyrazinyl derivative **11j**.

In spite of having good binding and functional potency at the target, physicochemical parameters within the optimal range for CNS drug candidates and, in some cases, LLE values approaching 5, compounds showed high human microsomal intrinsic clearance and, in some cases, modest aqueous solubility. Thus, our optimization efforts turned to other regions in the scaffold as the structure activity requirements at the amide region were apparently tight.

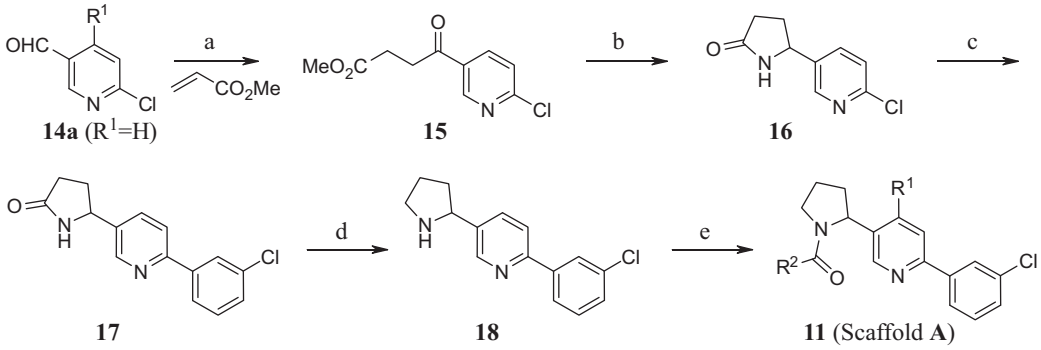

Scheme 1. Synthesis of analogs in scaffold **A** (R^1 = H). Reagents and conditions: (a) NaCN, DMF, rt, 93%; (b) NH_4OAc, $NaCNBH_3$, MeOH, rt, 42%; (c) *m*-Cl-PhB$(OH)_2$, $Pd(PPh_3)_4$, Na_2CO_3, DME, water, 70 °C, 73%; (d) BH_3·THF, reflux, 78%; (e) R^2CO_2H, EDCI, DMAP, DCM, 70–80%.

Table 1
Structure–activity relationships and physicochemical properties for a series of scaffold **A** analogs

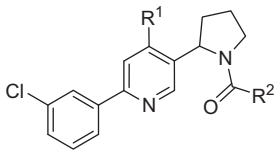

Scaffold **A**

Compd	R^1	R^2	*c* Log *P*	PSA (Å^2)	IC_{50} (nM)	K_i (nM)	LLE[a]	hCL_{int}[b] (L/min)	Solubility[c] (μM)	pK_a
11a	H		4.5	33	8	89	3.6	3.0	24	3.6
11b	H		3.5	46	5	140	4.8	3.8	35	—
11c	H		3.5	46	9	110	4.5	1.6	210	3.6
11d	H	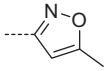	3.5	59	41	540	3.9	—	100	3.5
11e	H		3.1	59	74	540	4.0	3.3	230	3.4
11f	H		3.2	33	23	360	4.4	—	190	—
11g	Me		3.9	46	14	19	4.0	5.2	18	—
11h	Me		3.9	46	2	30	4.8	35	170	4.2
11i	Me	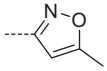	4.0	59	3	150	4.5	38	100	4.2
11j	Me		3.1	59	10	120	4.9	3.3	230	4.1
11k	Me		3.1	59	84	180	4.0	5.3	170	—
11l	Me		3.1	59	110	290	3.9	—	240	—
11m	Me		4.1	46	140	370	2.8	—	160	—
11n	Me		4.1	46	140	540	2.8	—	200	—
11o	Me		4.1	46	68	180	3.1	—	200	—
11p	Me		3.7	33	11	15	4.3	5.3	140	—
11q	Me	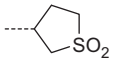	2.0	67	1900	7000	3.7	—	220	—
11r	Me	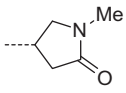	4.0	53	10,000	16,000	1.0	—	240	—
11s	OMe		3.9	55	8	20	4.2	1.7	8.7	5.0
11t	OMe		3.6	42	8	12	4.5	—	54	—

Table 1 (*continued*)

Compd	R^1	R^2	*c* Log *P*	PSA (Å^2)	IC_{50} (nM)	K_i (nM)	LLE[a]	hCL_{int}[b] (L/min)	Solubility[c] (μM)	pK_a
11u	OH		3.5	53	680	7800	2.7	—	210	2.8
11v			3.3	66	2400	13,000	2.3	—	12	—

[a] LLE = pIC_{50}-*c* Log *P*.
[b] Human hepatic blood flow = 1.5 L/min.[23]
[c] Kinetic solubility.[24]

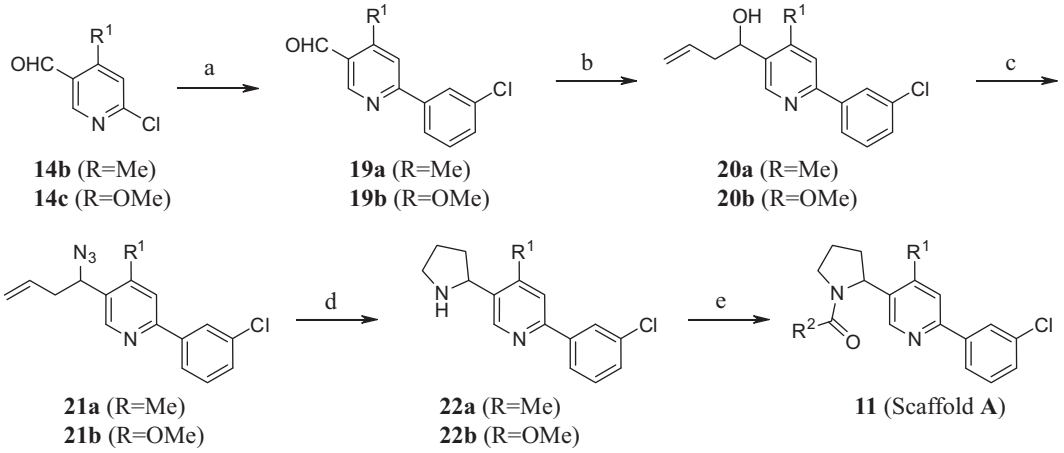

Scheme 2. Synthesis of analogs in scaffold **A** (R^1 = Me or OMe). Reagents and conditions: (a) *m*-Cl-PhB$(OH)_2$, $Pd(PPh_3)_4$, Na_2CO_3, toluene, water, 50%; (b) CH_2=$CHCH_2MgBr$, THF, 70%; (c) DPPA, DBU, toluene, 90 °C, 85%; (d) BH_3–DMS, cyclohexene, THF, 75%; (e) R^2CO_2H, EDCI, DMAP, DCM, 30–70%.

The effect of varying the aryl group on position 6 of the pyridine core on analogs within scaffold **A** was investigated next, and the results are shown in Table 2. At the outset, our goal was to identify a less lipophilic substituent than the 3-chlorophenyl group, seeking to improve the overall physicochemical properties in our target compounds. The only analogs made were those containing the preferred amides R^2 (vide supra). These studies showed that the 3-chlorophenyl substituent afforded an optimal balance between in vitro potency at the target and physicochemical properties. A simple switch to the fluoro analog showed a 10-fold loss of potency (**23a** and **23b**). The 3-chloro-5-fluorophenyl disubstituted analogs **23e** and **23f** were about 20 times less potent than the 3-chlorophenyl, but five times more potent than the 3,5-difluorophenyl substituent, further illustrating the preference for the chloro group. Aqueous solubilities were not improved comparing with the 3-chlorophenyl analogs. A number of heterocyclic replacements were explored. The most potent analogs obtained incorporated a 3-methyl-2-pyridyl group, albeit these were still 10-fold weaker than the 3-chlorophenyl. While LLE values approached 5 for compounds **23g** and **23h**, mainly due to their low *c* Log *P*, these compounds had relatively weak potencies.

Seeking to further optimize these analogs in terms of physicochemical properties and improving microsomal stability, we explored the effects of introducing fluorine or hydroxy substituents on the pyrrolidine ring, while using optimal fragments on the other regions. These hydroxy- and fluoro-pyrrolidine derivatives were prepared via a cyanomorpholine intermediate, an acyl anion equivalent, as shown in Scheme 3.[22] The cyanomorpholine was prepared by reacting the previously described aldehyde **19a** (R^1 = Me) with morpholine in the presence of sodium cyanide. This intermediate **24** was alkylated with epibromohydrin yielding the epoxide **25**, which was subsequently treated with 7 N methanolic ammonia at 60 °C. During the course of this reaction, the ketone intermediate was liberated and spontaneously cyclized to the pyrroline **26**. Sodium borohydride reduction of **26** followed by amide coupling produced the hydroxypyrrolidine **27** as a ca. 1:1 mixture of diastereomers. Fluorination of intermediate **27** with DAST followed by amide coupling gave rise to the fluoropyrrolidine **28**, also as a 1:1 mixture of isomers. Amidation of **27** or **28** under standard conditions yielded the final amide analogs **29a–f**.

The results obtained with this strategy are shown in Table 3. Hydroxy substitution rendered compounds **29a–c** having *c* log *P* values greater than 1 unit lower than the corresponding unsubstituted analog, bringing the lipophilicity of these compounds closer to preferred values for CNS drugs.[21] Human microsomal intrinsic clearance was also improved, albeit at the cost of a 10-fold loss in potency at the target. Fluoro substituted compounds **29d–f** had *c* log *P* values similar to the corresponding unsubstituted analogs and also showed weaker in vitro potencies as mGlu5 NAMs. In vitro clearance and LLE values did not improve.

In order to gain further insight on the structure–activity relationships of the compounds made, an examination of the pIC_{50} versus pK_i was undertaken (Fig. 4). A linear relationship between the functional and binding potencies of these analogs was observed, showing that under the assay conditions used for these in vitro screens the binding affinity K_i was consistently shifted ca. one log unit to the right (weaker values) compared to IC_{50} values. High potency was achieved with compounds having *c* Log *P* values in the 3.5–4.5 range. Compounds with LLEs near five were obtained with *c* Log *P* values more appropriate for CNS drugs, albeit their potency was weak. This indicated the lead optimization within this series required the need for a compromise between potency and lipophilicity, and limited the potential scope of this scaffold.

Based on the argument above and the balanced properties shown for racemic **11g** (Table 1), we selected this compound for resolution and further in vivo brain and plasma exposure studies

Table 2
Structure–activity relationships and physicochemical properties for a series of scaffold **A** analogs

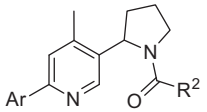

Compound	Ar	R^2	*c* Log *P*	PSA (Å^2)	IC_{50} (nM)	K_i (nM)	LLE[a]	Solubility[b] (μM)
23a	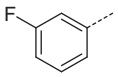		3.4	46	30	110	4.1	100
23b	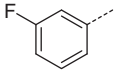		2.6	59	120	1100	4.3	52
23c	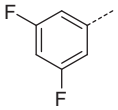		3.5	46	570	360	2.7	69
23d	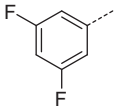		2.7	59	2000	2400	3.0	77
23e	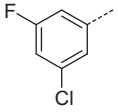		4.1	46	74	150	3.0	–
23f	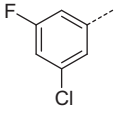		3.3	59	390	800	3.1	54
23g	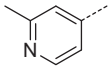		2.3	59	120	840	4.6	–
23h	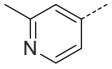		1.5	72	370	–	4.9	170

[a] LLE = pIC_{50}-*c* Log *P*.
[b] Kinetic solubility.[24]

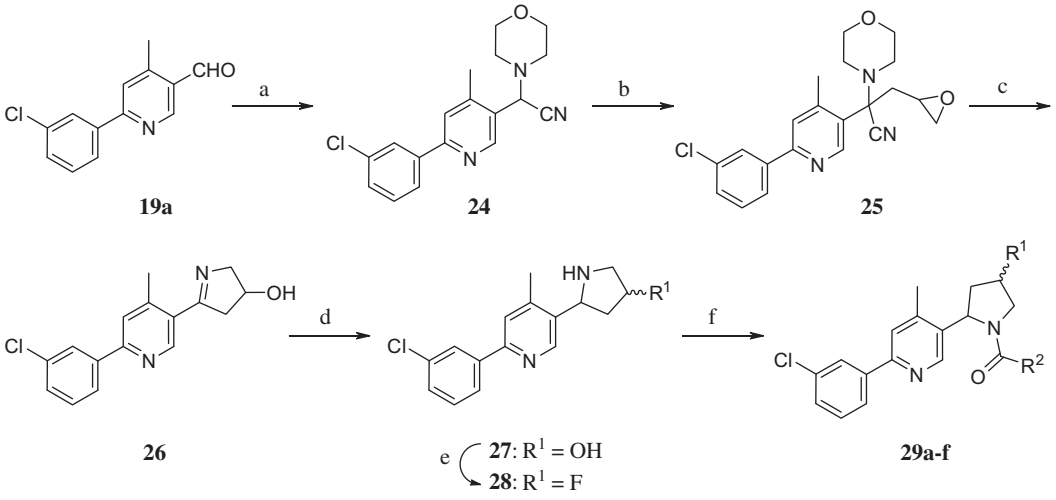

Scheme 3. Synthesis of substituted pyrrolidine analogs. Reagents and conditions: (a) morpholine, NaCN, PTSA, THF, 90%; (b) NaH, epibromohydrin, DMF, 60%; (c) NH_3, MeOH, reflux, 40%; (d) $NaBH_4$, EtOH, H_2O, 99%; (e) DAST, DCM, 26–58%; (f) R^2CO_2H, EDCI, DMAP, DCM, 30–50%.

Table 3
Structure–activity relationships and physicochemical properties for a series of substituted pyrrolidines

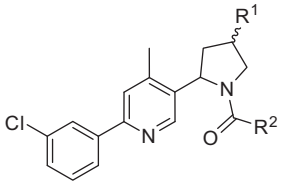

Compd	R^1	R^2	*c* Log *P*	PSA (A^2)	IC_{50} (nM)	K_i (nM)	LLE[a]	hCL_{int}[b] (L/min)
29a	OH		2.7	66	80	230	4.4	0.9
29b	OH		2.8	53	320	570	3.7	—
29c	OH		1.9	79	320	3000	4.6	1.6
29d	F		3.9	46	94	100	3.1	7.1
29e	F		3.7	33	140	130	3.2	—
29f	F		3.1	59	120	260	3.8	2.6

[a] LLE = pIC_{50}-*c* Log *P*.
[b] Human hepatic blood flow = 1.5 L/min.[23]

on the preferred enantiomer, once identified. Upon resolution, we found that mGlu5 activity resided essentially in one enantiomer, the absolute configuration of which has been arbitrarily assigned. The eutomer obtained from the chiral chromatographic separation (compound **30**) showed an eudismic ratio of 46 and was potent in both binding and functional mGlu5 assays (K_i = 12 nM and IC_{50} = 17 nM, respectively), had good aqueous solubility at pH 7.4 (44 μg/mL), and reasonable passive membrane permeability (P_{APP} of 15×10^{-6} cm/s, estimated using a PAMPA assay). Experimental Log $D_{7.4}$ was 4.3, in line with high rat and human plasma protein binding (rPPB = 99.5% and hPPB = 99.6%, respectively) and a low rat brain free fraction (UB_{BR} = 0.7%). A single dose–exposure study in Sprague–Dawley rats revealed that 1 h after an oral dose of 10 mg/kg (formulated in 20% w/v aqueous β-hydroxypropylcyclodextrin), **30** had moderate plasma and brain concentrations, and a brain/plasma ratio of 0.8. Free drug concentrations of **30** in plasma and brain (both 1 nM) were similar to its CSF concentration (3 nM), albeit below the mGlu5 NAM IC_{50} or K_i values at this oral dose, a likely consequence of extensive hepatic metabolism.

In summary, while several mGlu5 NAMs have achieved clinical proof-of-concept for a number of indications, the discovery of novel chemotypes lacking the alkyne functionality remains a challenge. We discovered a series of 6-aryl-3-pyrrolidinylpyridines as structurally novel, non-alkyne negative allosteric modulators of the mGlu5 receptor. Functional and binding potency correlate well in the in vitro screens used, SAR was found to be tractable, and the switch to either positive or silent (PAMs or SAMs, respectively) allosteric modulators reported in other series has not been observed in this chemotype.[15b,c] At the amide moiety, five-membered heterocycles are preferred, while the 3-chlorophenyl group appears to be preferred and difficult to replace. Substitution in the 4-position of the pyridine core with a methyl or methoxy group yielded compounds with superior in vitro potency, and reasonable CNS partition profiles and physicochemical properties. Furthermore, the SAR observed in these pyridine derivatives matches

Compd	Structure	IC_{50} (nM)	K_i (nM)	LLE[a]	Brain (nM)	Plasma (nM)	CSF (nM)	rPPB[b] (%)	rUB_{BR}[c] (%)
30	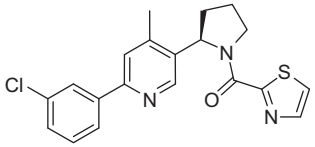	17	12	3.9	133	162	3	99.5	0.7

[a] LLE = pIC_{50}-*c* Log *P*.
[b] Rat plasma protein binding.[25]
[c] Rat brain free fraction.[25]

Additional exploration of pharmacokinetic properties of multiple derivatives in this series did not afford the appropriate peripheral or central drug exposure profiles to support once daily oral administration in human. The strategy of exploring alternate improved scaffolds is ongoing.

observations recently reported for related five-membered heterocyclic ring systems (e.g., oxadiazoles and tetrazoles).[15a,b] Follow

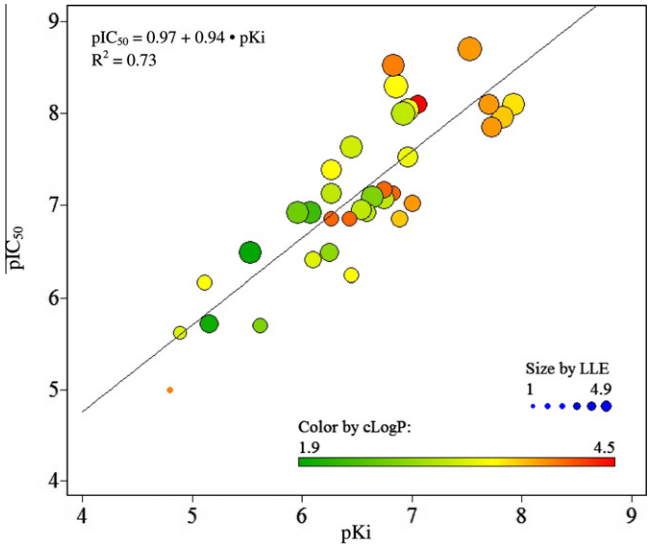

Figure 4. Representation of pIC_{50} versus pK_i for analogs in Tables 1–3.

up efforts expanding the six-membered heterocyclic central ring to diverse heterocyclic systems will be reported in future communications.

Acknowledgements

We are grateful to Drs. Mark Hayward, Qing-Ping Han, Chi Zhang and Xu Zhang, in the CPS Department, for determinations of physicochemical properties and the resolution of compound **11g**, to Christina L. Bonvicino and Xiaosui Pu for in vitro pharmacology determinations and to Dr. Albert J. Robichaud for his support during this work and for helpful comments to this manuscript.

References and notes

1. Stahl, S. M. *Stahl's Essential Psychopharmacology*, 3rd ed.; Cambridge University press: 2008; Watkins, J. C. *Biochem. Soc. Trans.* **2000**, *28*, 297.
2. Foord, S. M.; Bonner, T. I.; Neubig, R. R.; Rosser, E. M.; Pin, J. P.; Davenport, A. P.; Spedding, M.; Harmar, A. J. *Pharmacol. Rev.* **2005**, *57*, 279.
3. G Protein-Coupled Receptors in Drug Discovery. In *Taylor & Francis*; Lundstrom, K. H., Chiu, M. L., Eds.; CRC Press, 2006; Behan, D. P.; Chalmers, D. T. *Nat. Rev. Drug Discov.* **2002**, *1*, 599.
4. (a) Schoepp, D. D.; Conn, P. J. *Trends Pharmacol. Sci.* **1993**, *14*, 13; (b) Schoepp, D. D. *Neurochem. Int.* **1994**, *24*, 439; (c) Bordi, F.; Ugolini, A. *Prog. Neurobiol.* **1999**, *59*, 55.
5. Topiol, S.; Sabio, M.; Uberti, M. *Neuropharmacology* **2011**, *60*, 93.
6. Conn, P. J.; Christopoulos, A.; Lindsley, C. W. *Nat. Rev. Drug Discovery* **2009**, *8*, 41.
7. (a) Ritzen, A.; Mathiesen, J. M.; Thomsen, C. *Basic Clin. Pharmacol. Toxicol.* **2005**, *97*, 202; (b) Kew, J. N. *Pharmacol. Ther.* **2004**, *104*, 233.
8. Porter, R. H. P.; Jaeschke, G.; Spooren, W.; Ballard, T. M.; Büttelmann, B.; Kolczewski, S.; Peters, J.-U.; Prinssen, E.; Wichmann, J.; Vieira, E.; Mühlemann, A.; Gatti, S.; Mutel1, V.; Malherbe, P. *J. Pharmacol. Exp. Ther.* **2005**, *315*, 711.
9. (a) Dekundy, A.; Gravius, A.; Hechenberger, M.; Pietraszek, M.; Nagel, J.; Tober, C.; van der Elst, M.; Mela, F.; Parsons, C. G.; Danysz, W. *J. Neural. Transm.* **2010**. doi:10.1007/s00702-010-0526-0. Published online on December 16, 2010; (b) Phan, K. L.; Fitzgerald, D. A.; Cortese, B. M.; Seraji-Bozorgzad, N.; Tancer, M. E.; Moore, G. J. *Neuroreport* **2005**, *16*, 183; (c) Mathew, S. J.; Price, R. B.; Charney, D. S. *Am. J. Med. Genet. C Semin. Med. Genet.* **2008**, *148C*, 89; (d) Breysse, N.; Baunez, C.; Spooren, W.; Gasparini, F.; Amalric, M. *J. Neurosci.* **2002**, *22*, 5569.
10. Marin, J. C.; Goadsby, P. J. *Expert Opin. Investig. Drugs* **2010**, *19*, 555.
11. Zerbib, F.; Keywood, C.; Strabach, G. *Neurogastroenterol. Motil.* **2010**, *22*, 859.
12. Jacquemont, S.; Curie, A.; des Portes, V.; Berry-Kravis, E.; Hagerman, R. J.; Ramos, F.; Cornish, K.; He, Y.; Paulding, C.; Torrioli, M. G.; Neri, G.; Chen, F.; Hadjikhani, N.; Martinet, D.; Meyer, J.; Beckmann, J. S.; Delange, K.; Brun, A.; Bussy, G.; Gasparini, F.; Hilse, T.; Floesser, A.; Branson, J.; Bilbe, G.; Johns, D.; Gomez-Mancilla, B. American Society of Human Genetics 60th Annual Meeting. Nov 2–6, 2010; Washington DC, US, 2010.
13. Berg, D.; Godau, J.; Trenkwalder, C.; Eggert, A.; Csoti, I.; Storch, A.; Gasparini, F.; Hariry, S.; Vandermeulebroecke, M.; Johns, D.; Gomez-Mancilla, B. *Mov. Disord.* **2010**, *25*(Suppl. 2), S290.
14. Development of ADX10059 Ended for Long-term Use. http://www.add-expharma.com/press-releases/press-release-details/article/development-of-adx10059-ended-for-long-term-use/ accessed on October 15, 2010.
15. (a) Wágner, G.; Wéber, C.; Nyéki, O.; Nógrádi, K.; Bielik, A.; Molnár, L.; Bobok, A.; Horváth, A.; Kiss, B.; Kolok, S.; Nagy, J.; Kurkó, D.; Gál, K.; Greiner, I.; Szombathelyi, Z.; Keserű, G. M.; Domány, G. *Bioorg. Med. Chem. Lett.* **2010**, *20*, 3737; (b) Lamb, J. P.; Engers, D. W.; Niswender, C. M.; Rodriguez, A. L.; Venable, D. F.; Conn, P. J.; Lindsley, C. W. *Bioorg. Med. Chem. Lett.* **2011**, *21*, 2711; (c) Graven Sams, A.; Mikkelsen, G. K.; Brodbeck, R. M.; Pu, X.; Ritzén, A. *Bioorg. Med. Chem. Lett.* **2011**. doi:10.1016/j.bmcl.2011.03.103.
16. Geometry optimizations were conducted using ChemBio3D Ultra 12.0, interfaced to GAMESS, using the HF method, basis set 6–31G, wave function R-closed shell and Pople exponent, which is distributed by CambridgeSoft of 100 Cambridge Park Drive, Cambridge, MA 02140.
17. Jimenez, H. N.; Li, G.; Doller, D.; Grenon, M.; White, A. D.; Guo, M.; Ma, G. WO 2010011570.
18. Stetter, H.; Schreckenberg, M.; Wiemann, K. *Ber.* **1976**, *109*, 541.
19. The structures of all final compounds made were confirmed using low resolution mass spectrometry. For representative examples of final analogs within a series, structures were confirmed using nuclear magnetic resonance (NMR), as well as low resolution mass spectrometry. Purity of all final products was determined to be >95% based on their LC–MS trace using ELSD or UV detection in the range of 240–400 nm, as well as at a single 254 nm wavelength. Purifications were carried out either on a preparative thin layer chromatography plate or on a reversed phase liquid chromatography/mass spectrometry (RP-HPLC/MS) purification system. Flow rate: 100 mL/min. Mobile phase additive: 48 mM of ammonium formate. Column: Inertsil® C18, 30 × 50 mm, 5 μm particle size.
20. (a) The cDNA for human metabotropic glutamate receptor 5 was a generous gift from S. Nakanishi (Kyoto University, Kyoto, Japan). The hmGluR5 was stably expressed in a HEK 293 cell line and grown in Dulbecco's Modified Eagle Medium (DMEM) (Invitrogen, Carlsbad, CA) with supplements (10% bovine calf serum, 4 mM glutamine, 100 units/mL penicillin, 100μg/mL streptomycin and 0.75 mM G1418) at 37 °C, 5% CO_2. Twenty-four hours prior to assay, cells were seeded into 384-well black wall microtiter plates coated with poly-Dlysine. Just prior to assay, media was aspirated and cells dye-loaded (25 μL/well) with 3 μM 20 Fluo-4/ 0.01% pluronic acid in assay buffer (Hank's Balanced Saline Solution (HBSS)): 150 mM NaCl, 5 mM KCl, 1 mM $CaCl_2$, 1 mM $MgCl_2$, plus 20 mM *N*-2-hydroxyethylpiperazine-*N*′-2-ethanesulfonic acid (HEPES), pH 7.4, 0.1% bovine serum albumin (BSA) and 2.5 mM probenecid) for 1 h in 5% CO_2 at 37 °C. After excess dye was discarded, cells were washed in assay buffer and layered with a final volume equal to 25 μL/well. Basal fluorescence is monitored in a fluorometric imaging plate reader (FLIPR, Molecular Devices, Sunnyvale, CA) with an excitation wavelength of 488 nm and an emission range of 500–560 nm. Laser excitation energy was adjusted so that basal fluorescence readings were approximately 10,000 relative fluorescent units. Cells were stimulated with an EC_{20} or an EC_{80} concentration of glutamate in the presence of a compound to be tested, both diluted in assay buffer, and relative fluorescent units were measured at defined intervals (exposure = 0.6 s) over a 3 min period at room temperature. Basal readings derived from negative controls were subtracted from all samples. Maximum change in fluorescence was calculated for each well. Concentration–response curves derived from the maximum change in fluorescence were analyzed by nonlinear regression (Hill equation). A negative modulator can be identified from these concentration–response curves if a compound produces a concentration dependent inhibition of the EC_{80} glutamate response.; (b) Binding assays were performed as described in [O'Brien, J. A.; et al. *Mol Pharmacol.* **2003**, *64*, 731] with slight modifications. Briefly, after thawing, the membrane homogenates were resuspended in 50 mM Tris–HCl, 0.9% NaCl binding buffer at pH 7.4 to a final assay concentration of 40 μg protein/well for [^{3}H] 2-methyl-6-phenylethynyl-pyridine ([^{3}H] MPEP, American Radiolabeled Chemicals, Inc., St. Louis, MO) filtration binding. Incubations included 5 nM [^{3}H]-MPEP, membranes and either buffer or varying concentrations of compound. Samples were incubated for 60 min at room temperature with shaking. Non-specific binding was defined with 10 μM MPEP. After incubation, samples were filtered over a GF/C filter (presoaked in 0.25% polyethyleneimine (PEI)) and then washed four times using a Tomtec® Harvester 96® Mach III cell harvester (Tomtec, Hamden, CT) with 0.5 mL ice-cold 50 mM Tris–HCl (pH 7.4). IC_{50} values were derived from the inhibition curve and K_i values were calculated according to the Cheng and Prusoff equation of $K_i = IC_{50}/(1 + [L]/K_d)$ described in [Cheng, Y.; Prusoff, W.H. *Biochem. Pharmacol.* **1973**, *22*, 3099] where [L] is the concentration of radioligand and K_d is its dissociation constant at the receptor, derived from the saturation isotherm.
21. Shaffer, C. L. *Annu. Rep. Med. Chem.* **2010**, *43*, 55. and references cited therein.
22. Hecht, S. S.; Chen, C. B.; Hoffmann, B. *J. Med. Chem.* **1980**, *23*, 1175.
23. Determination of metabolic stability in liver microsomes. This study was conducted by incubating 1 μM concentration of test compounds at 37 °C in pooled male rat or pooled human liver microsomes (0.5 mg/mL) in 0.1 M potassium phosphate buffer (pH 7.4) supplemented with NADPH-regenerating system (1.3 mM $NADP^+$, 3 mM $MgCl_2$, 3.5 mM glucose-6-phosphate, and 4 units glucose-6-phosphate dehydrogenase). Aliquots were taken at 0.25, 5, 15, 30 and 60-minute time points. The aliquots were added to a 96-well plate containing an equal volume of acetonitrile in order to terminate the reaction. The samples were vortexed and centrifuged at 3000 rpm for 15 min. A known volume of internal standard was added to the supernatant. The samples were injected in an LC–MS/MS system to monitor the disappearance of the parent

compound. The half-life was measured by plotting the log of the remaining compound versus time. The in vitro half-life data were used to calculate the intrinsic clearance (CLint), according to the equation shown below:

$$\mathrm{CLint} = 0.693 \times \frac{1}{T_{1/2}(min)} \times \frac{\text{g liver weight}}{\text{kg body weight}} \times \frac{\text{mL incubation}}{\text{mg microsomal protein}} \times \frac{\text{mg microsomal protein}}{\text{g liver weight}} \times \text{kg body weight}$$

where, liver weight is 20 g/kg in human and 45 g/kg in rat, and body weight is 70 kg for human and 250 g in rat. In this equation, it was assumed that 1 g of liver contains 45 mg of microsomal protein and the binding of the drug to microsomal proteins was assumed to be zero, hence the unbound drug fraction, $f_{u,mic} = 1$.

24. Kinetic solubilities were measured from 10 mM DMSO stock solution of the test compound (300 μL) diluted with 2 × 200 μL of 25 mM potassium phosphate buffer in a Titer plate shaker at a speed of 1.8 for 4 h. The supernatant was analyzed by using a Waters Acquity UPLC system (Column: Acquity UPLC BEH C-18, 1.7 μm 2.1 × 50 mm column and PDA detector at 254 nm for quantitation) with a gradient (mobile phase A: 2% w/v ammonium formate and 20% acetonitrile in water, mobile phase B: 100% acetonitrile) for 2 min.
25. Human and rat protein binding studies, and rat brain homogenate free fraction studies were determined by using a 96-well format equilibrium dialyzer (HTD96b, Catalog# 1006, www.htdialysis.com). Test compounds (10 μM) were spiked into serum from human or rat and dialyzed against phosphate buffered saline (pH 7.4) via a >5000 molecular weight dialysis membrane for 2.5 h in an incubator set to maintain 37 °C with 5% CO_2. The dialysis block was placed on an orbital shake. After 2.5 h incubation, buffer and serum samples (or brain homogenate samples) were collected and transferred into a 96-well matrix plate with tube inserts. Internal standards were added and the samples were vortexed and mixed, and analyzed by LC–MS/MS.